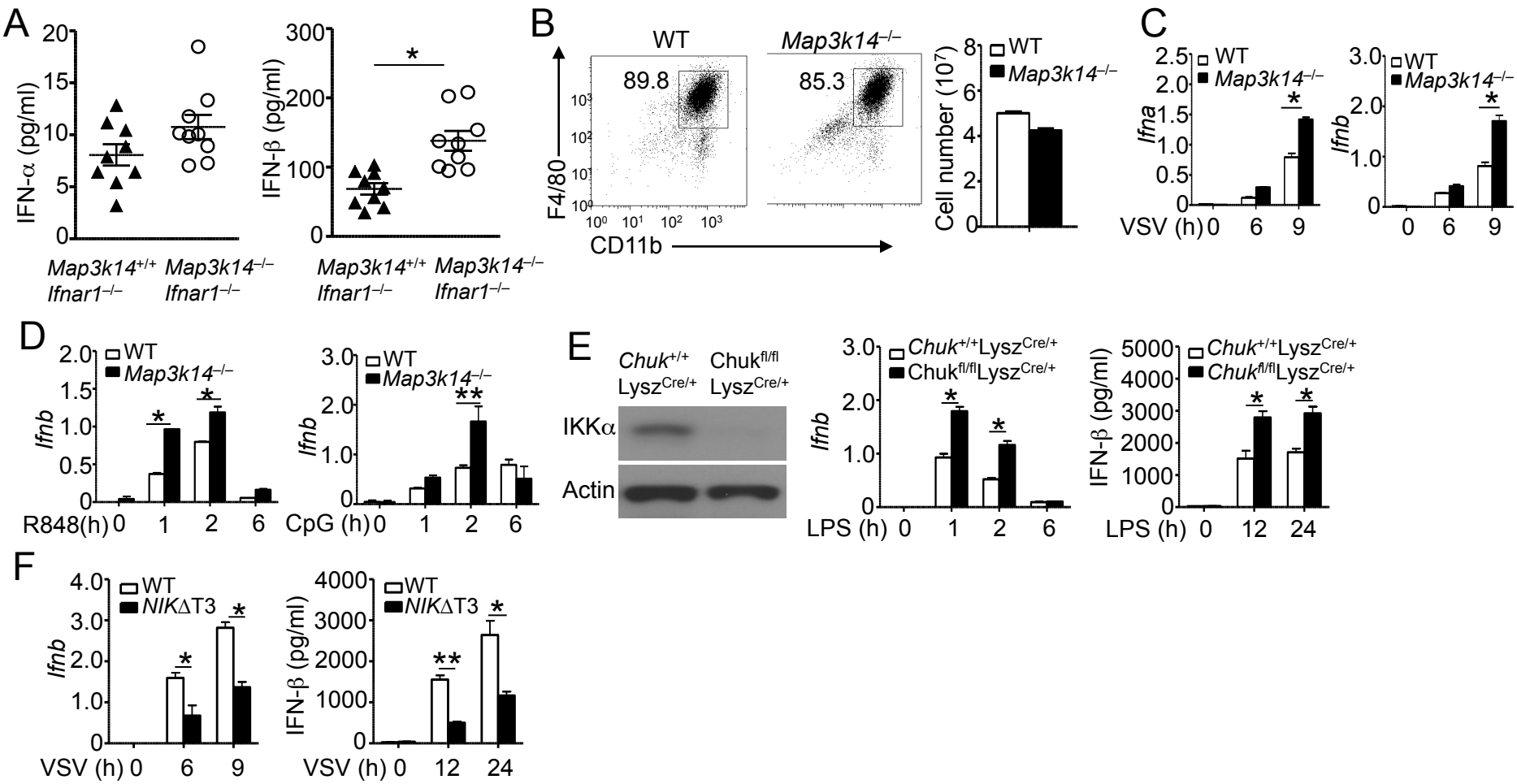

Figure S1. NIK negatively regulates type I IFN production. **Related to Figure 1.**
(A) Wild-type (WT) and *Map3k14*$^{-/-}$ mice, bred to the *Rag1*$^{-/-}$ */Ifnar1* $^{-/-}$ background, were infected i.v. with VSV (2×10^7 PFU/ mouse). Serum concentrations of IFN-α and IFN-β at 12 h of infection were measured by ELISA. (B) Flow cytomery analysis of the percentage (left) and absolute number (right) of macrophages (F4/80$^+$CD11b$^+$) generated through *in vitro* differentiation of bone marrow cells from WT or *Map3k14*$^{-/-}$ mice. (C) QPCR analysis of *Ifna* and *Ifnb* mRNA levels (fold relative to the *Actin* mRNA amount) in WT and *Map3k14*$^{-/-}$ BMDMs infected with VSV for the indicated time periods.(D) QPCR analysis of *Ifnb* relative mRNA levels in WT and *Map3k14*$^{-/-}$ BMDMs stimulated with R848 and CpG. Data are presented as mean ± S.D. and representative of 3 independent experiments. (E) BMDMs derived from *Chuk*$^{+/+}$Lys^{Cre} and Chuk$^{fl/fl}$Lys^{Cre} mice were subjected to IKKα immunoblot (upper) or stimulated with LPS and then subjected QPCR analysis of *Ifnb* mRNA and ELISA of IFN-β (lower).(F) QPCR analysis of *Ifnb* mRNA (left) and ELISA of IFN-β protein (right) levels in WT and NIKΔT3 BMDMs infected with VSV. *P<0.05 and **P<0.01.

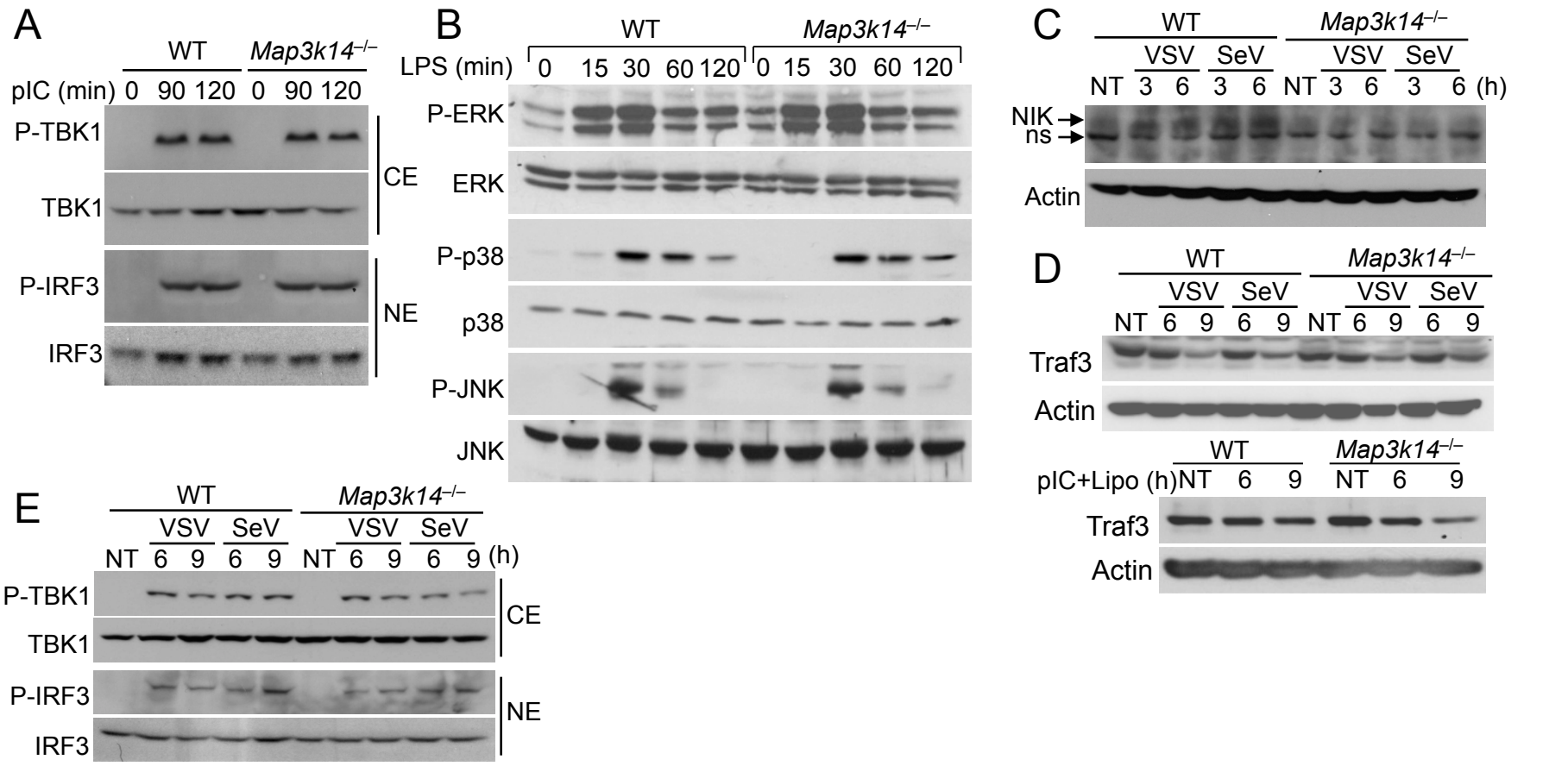

Figure S2. Deficiency in the NIK pathway does not influence the activation of TBK1 and MAP kinases or the differentiation of macrophages. **Related to Figure 3.**

(A) Immunoblot analysis of phosphorylated (P-) and total TBK1 and IRF3 in WT or *Map3k14*$^{-/-}$ BMDMs stimulated with poly(I:C). (B) Immunoblot analysis of the phosphorylated (P-) and total proteins of the indicated MAP kinases in WT and *Map3k14*$^{-/-}$ BMDMs stimulated with LPS for the indicated time periods. (C) Immunoblot analysis of the indicated proteins in whole-cell lysates of WT and *Map3k14*$^{-/-}$ MEFs infected with VSV or SeV for the indicated times. 4 times as much protein lysates as the other immunoblots were loaded for visualizing NIK. A non-specific (ns) band is indicated. (D) Immunoblot analysis of TRAF3 degradation induced by viruses and liposome-delivered poly(I:C). (E) Immunoblot analysis of phosphorylated (P-) and total TBK1 and IRF3 in the cytoplasmic (CE) and nuclear (NE) extracts of WT and *Map3k14*$^{-/-}$ MEFs infected with VSV or SeV.

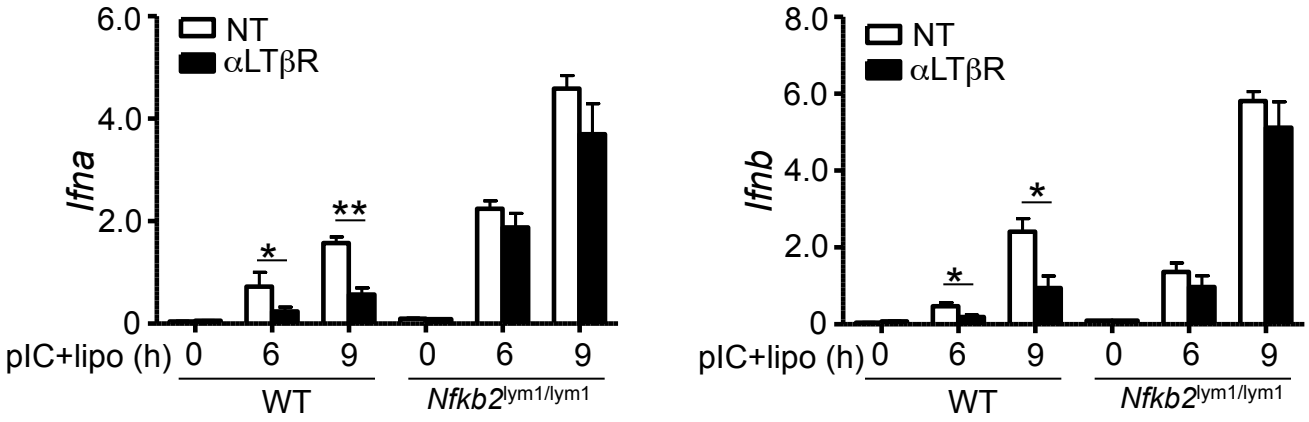

Figure S3. Pre-treatment of MEFs with a noncanonical NF-kB inducer inhibits IFN-I induction. Related to Figure 3.

WT and *Nfkb2*$^{lym1/lym1}$ MEFs were pretreated for 24 h with anti-LTbR (500 ng/ml), washed and rested for 8 h, and then stimulated with liposome-transfected poly(I:C) for the indicated time periods. Relative levels of *Ifna* and *Ifnb* mRNA were quantified by QPCR. Data are representative of two independent experiments. *P<0.05 and **P<0.01

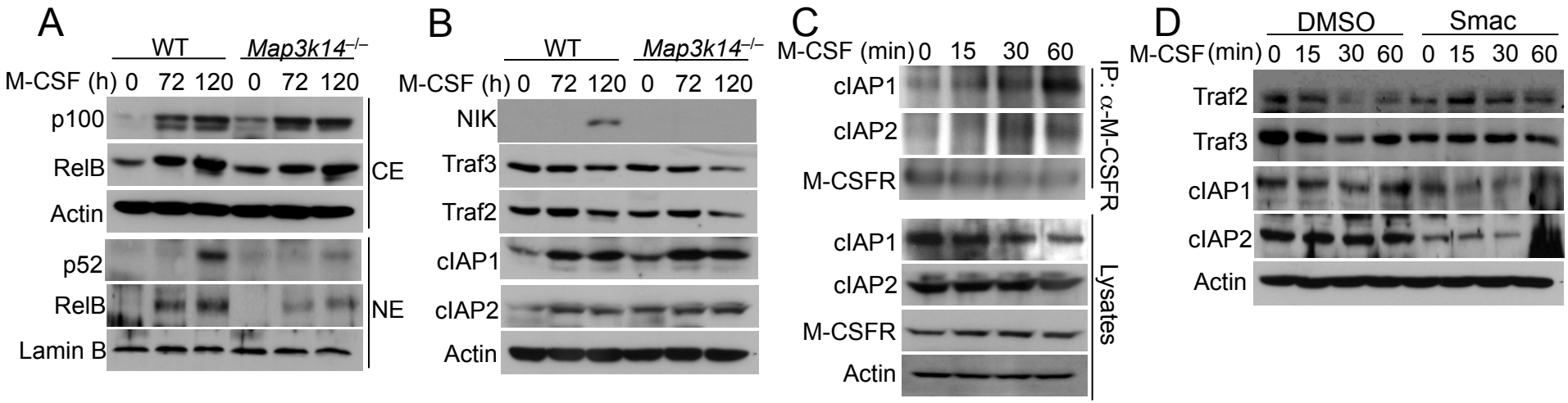

Figure S4. M-CSF-stimulated degradation of TRAF2 and TRAF3 requires c-IAP1 and c-IAP2. Related to Figure 4.
(A) Bone marrow cells were cultured with M-CSF (200 ng/ml) (M-CSF was added on day 0 and again on day 3). Immunoblot analysis of the indicated proteins in the cytoplasmic (CE) and nuclear (NE) extracts of bone marrow (BM) cells from WT and *Map3k14*$^{-/-}$ mice.
(B) Immunoblot analysis of the indicated proteins in cytoplasmic lysates of WT or *Map3k14*$^{-/-}$ bone marrow cells. Data are representative of three independent experiments.
(C) WT bone marrow cells were stimulated with M-CSF. M-CSFR complexes were isolated by IP from whole-cell lysates, and the M-CSFR-associated c-IAP1 and c-IAP2 were detected by IB (upper). Cell lysates were also directly subjected to IB (lower).
(D) Immunoblot analysis of the indicated proteins in the whole-cell lysates of WT bone marrow cells pretreated for 4 h with a c-IAP inhibitor, Smac mimetic (1 mM), or solvent control DMSO and then stimulated with M-CSF for the indicated time periods.

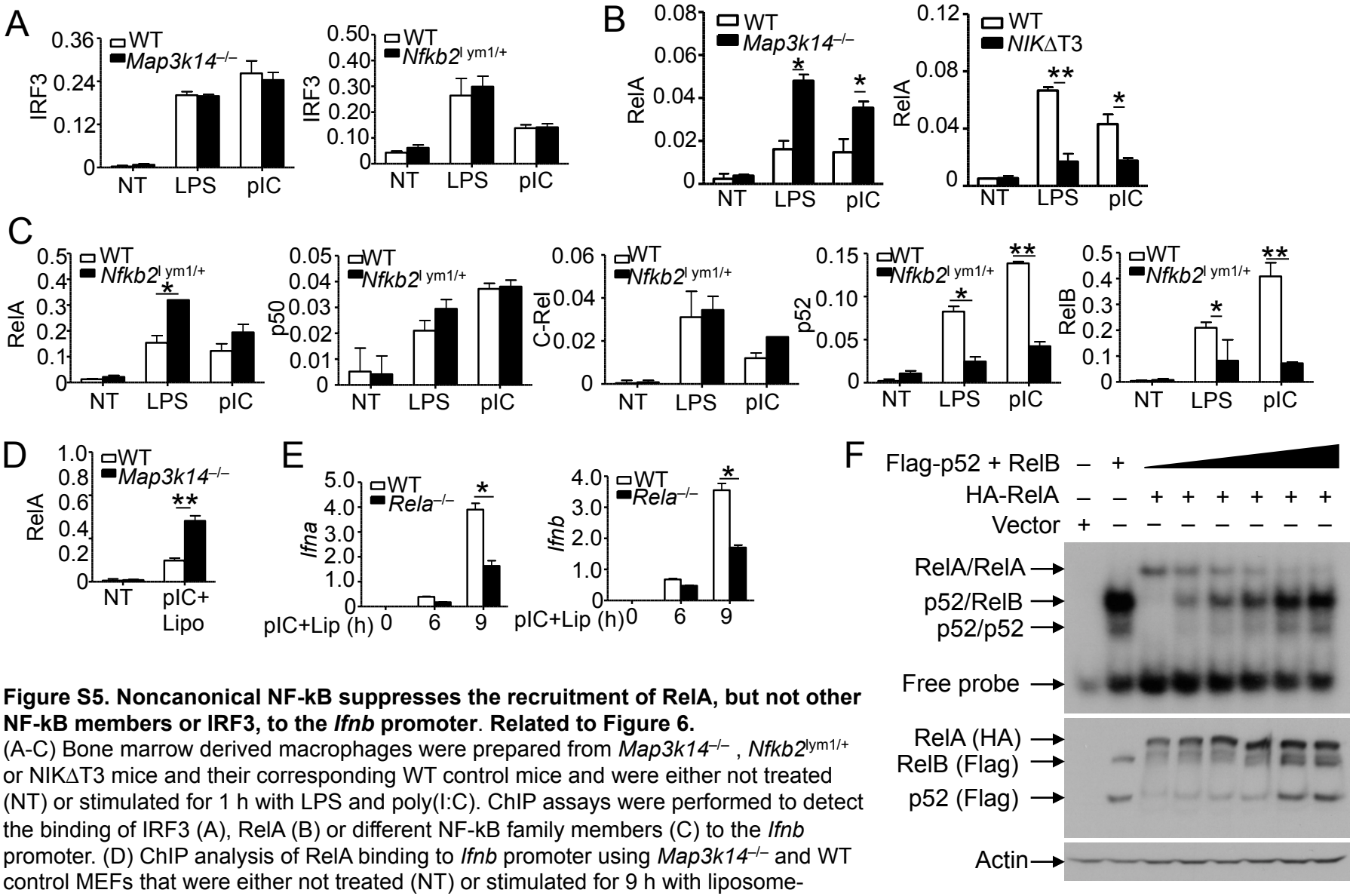

Figure S5. Noncanonical NF-kB suppresses the recruitment of RelA, but not other NF-kB members or IRF3, to the *Ifnb* promoter. **Related to Figure 6.**
(A-C) Bone marrow derived macrophages were prepared from *Map3k14*$^{-/-}$, *Nfkb2*$^{lym1/+}$ or NIKΔT3 mice and their corresponding WT control mice and were either not treated (NT) or stimulated for 1 h with LPS and poly(I:C). ChIP assays were performed to detect the binding of IRF3 (A), RelA (B) or different NF-kB family members (C) to the *Ifnb* promoter. (D) ChIP analysis of RelA binding to *Ifnb* promoter using *Map3k14*$^{-/-}$ and WT control MEFs that were either not treated (NT) or stimulated for 9 h with liposome-transfected poly(I:C). Data are presented as percentage of the total input DNA and representative of three independent experiments. (E) QPCR analysis of *Ifna* and *Ifnb* relative mRNA levels in wild-type and *Rela* $^{-/-}$ O MEFs stimulated with Lipofectamine-delivered poly(I:C). (F) HEK293 cells were transfected with the indicated doses of NF-kB members, and whole-cell lysates were subjected to EMSA using the *Ifnb* kB probe (upper) or immunoblot analysis (lower).

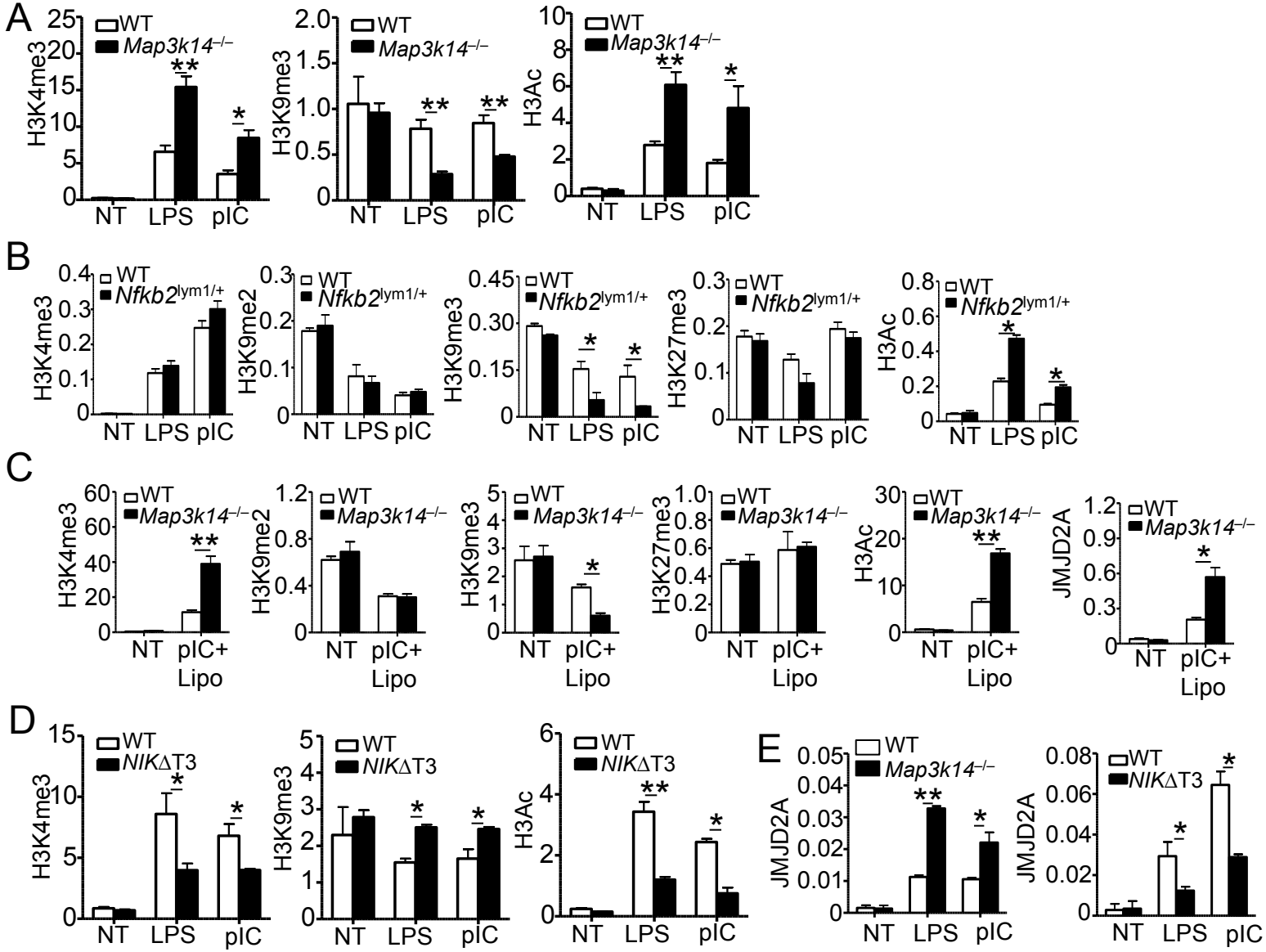

Figure S6. Noncanonical NF-kB pathway regulates histone modification at the *Ifnb* promoter. Related to Figure 7.
(A-D) ChIP analysis of histone modifications at the *Ifnb* promoter using the indicated mutant and WT control BMDMs stimulated for 1 h with LPS or poly(I:C) (A, B, and D) or the *Map3k14*$^{-/-}$ and WT control MEFs stimulated for 9 h with liposome-transfectedpoly(I:C) (C). The Y axis shows the level of chromatin DNA that was bound by modified histone 3, presented as percentage of total histone 3-bound DNA. (E) ChIP analysis of JMJD2A binding to the *Ifnb* promoter using *Map3k14*$^{-/-}$ (left) or NIKΔT3 (right) and WT control BMDMs stimulated for 1 h with LPS or poly(I:C). All histone modification level is normalized with total H3. The Y axis is percentage of total input DNA.

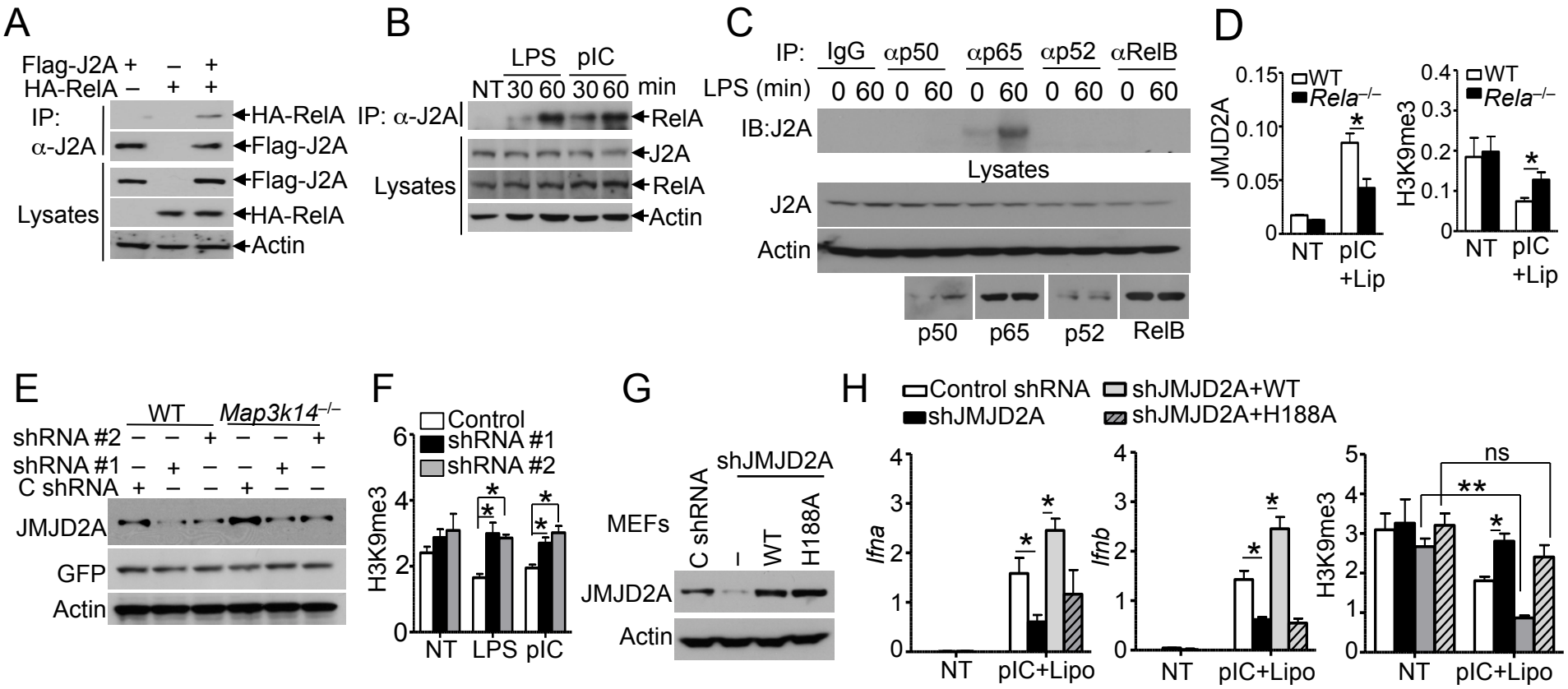

Figure S7. Potential role of RelA in mediating JMJD2A binding to the *Ifnb* promoter. Related to Figure 7.
(A) HEK293 cells were transfected with the indicated expression vectors. Cell lysates were subjected to IP using anti-JMJD2A (a-J2A) followed by IB to detect precipitated JMJD2A (J2A) and the co-precipitated RelA (top two panels). Cell lysates were also directly analyzed by IB (bottom three panels). (B) Whole-cell lysates of WT BMDMs, stimulated as indicated, were subjected to JMJD2A (J2A) IP, and the JMJD2A-associated RelA was detected by IB (top panel). Protein expression levels were analyzed by direct IB (bottom three panels). (C) Whole-cell lysates of WT BMDMs, stimulated with LPS, were subjected to the indicated IP followed by detecting NF-kB-associated JMJD2A (J2A) by IB (top panel). Protein expression was monitored by direct IB (bottom three panels). (D) WT and *Rela*$^{-/-}$ MEFs were either not treated (NT) or stimulated with lipofectamine-transfected poly(I:C) (pIC + Lip) for 9 h and subjected to ChIP assays to detect JMJD2A and H3K9me3 binding at the *Ifnb* protomoter. (E and F) WT and *Map3k14*$^{-/-}$ macrophages were infected with a GFP-expressing lentiviral vector (pGIPZ) encoding either a control luciferase shRNA (C shRNA) or two different JMJD2A shRNAs. GFP^{+} cells were sorted by FACS and subjected to immunoblot analysis to detect the JMJD2A knockdown efficiency and control protein expression (E) or ChIP analysis of H3K9me3 modification at the *Ifnb* promoter (F). (G and H) WT MEFs were infected with lentiviral vectors encoding a control shRNA (C shRNA) or a JMJD2A shRNA (shJMJD2A). The JMJD2A-knockdown cells were then rescued with an RNAi-resistant form of WT JMJD2A or a catalytically inactive JMJD2A mutant (H188A). The cells were subjected to JMJD2A immunoblot (G) or stimulated for 9 h with lipofectamine-transfected poly(I:C) and then subjected to IFN-I QPCR analysis (H, left two panels) or H3K9me3 ChIP assays (H, right panel). Data are representative of three independent experiments. *P<0.05 and **P<0.01.

Gene	Forward primer	Reverse primer
Ifna	AGTCCATCAGCAGCTCAATGAC	AAGTATTTCCTCACAGCCAGCAG
Ifnb	AGCTCCAAGAAAGGACGAACAT	GCCCTGTAGGTGAGGTTGATCT
Ifnb promoter (CHIP)	ATTCCTCTGAGGCAGAAAGGACCA	GCAAGATGAGGCAAAGGCTGTCAA

Table S1. The gene-specific primers used for real-time RT-PCR for detecting the indicated mouse mRNAs. Related to Experimental Procedures.

SUPPLEMENTAL EXPERIMENTAL PROCEDURES

Plasmids, antibodies, viruses, and reagents. The pcDNA expression vectors encoding FLAG-tagged p52 and RelB were from Addgene. pEF-p65-HA, FLAG-JMJD2A, and FLAG-IRF3 were provided by Drs. Lienhard Schmitz, Hsing Jien Kung, and Joseph S Pagano, respectively. Retroviral vectors encoding JMJD2A (pLPC-puro-FLAG-JMJD2A) and a catalytically inactive JMJD2A mutant (pLPC-puro-FLAG-JMJD2A H188A) were described previously (Mallette and Richard, 2012). A luciferase reporter driven by the *Ifnb* promoter (IFNβ-luc) was provided by Dr. Dimitris Thanos.

Antibody for murine p100/p52 (TB4) was from NCI. Antibodies for RelB (C-19), Lamin B (C-20), NIK (H248), TRAF2 (C-20), TRAF3 (C-20), cIAP1 (H83), cIAP2 (H85), IKKα (H744), TBK1 (108A429), IKKε (IKKi, H-116), p105/p50 (C-19), JMJD2A (D-9) and MCSFR (CSF-1R, H300) were from Santa Cruz Biotechnology. Antibody for Actin (C-4) was from Sigma; phospho-TBK1 (pTBK1, Ser172) (D52C2) was from Cell Signaling Technology; phospho-IRF3 was from Pierce; and phospho-IKKε (pIKKi, Ser172) (06-1340) was from Millipore. HRP-conjugated anti-HA (HA-7) and HRP-conjugated anti-FLAG (M2) were from Sigma-Aldrich. Fluorescence-labeled antibodies are listed in the section of flow cytometry and cell sorting. For ChIP assays, antibody for c-Rel (sc-71) was from Santa Cruz Biotechnology; antibodies for H3Ac (06-599), H3K4me3 (07-473), and H3K27me3 (07-449) were from Millipore; antibodies for H3K9me2 (ab1220), H3K9me3

(ab8898), G9a (ab40542), JMJD2A (ab105953), Jmjd2c (ab85454), Jmjd2d (ab93694) and Jmjd3 (ab85392) were from abcam. Other antibodies were as previously described(Chang et al., 2011).

VSV (Indiana strain) and VSV carrying a GFP gene (VSV-GFP) were provided by Glen Barber(Fernandez et al., 2002). A VSV variant harboring a point mutation in the M gene (AV1) was provided by John Bell (Stojdl et al., 2003). Viral stock was prepared and titered by infecting baby hamster kidney cells. Sendai virus was from Charles River laboratories. The JMJD2 inhibitor 5-carboxy-8HQ was from Calbiochem, LPS (derived from *Escherichia coli* strain 0127:B8) was from Sigma-Aldrich, poly(I:C) was from Amersham, recombinant murine MCSF was from Peprotech, and Lipofectamine was from Invitrogen.

Luciferase Reporter Gene Assays

HEK293 cells (2 x 10^5) were seeded into 24-well plates and transfected, by calcium phosphate precipitation, with the *Ifnb*-luc reporter plasmid along with the indicated cDNA expression vectors as well as the control pRL-TK promoter Renilla luciferase reporter. Luciferase assays were performed with a dual-specific luciferse assay kit (Promega). Firefly luciferase activities were normalized based on the Renilla luciferase activities.

EMSA

EMSA was performed as previously described (Maggirwar et al., 1997) using a

^{32}P-radiolabeled oligonucleotide probe covering the IFNβ κB element (pRD1-II):

5'-AACTGAAAGGGAGAACTGAAAGTGGGAAATTCCTCTGA-3'

SUPPLEMENTAL REFERENCES

Chang, M., Jin, W., Chang, J.H., Xiao, Y., Brittain, G.C., Yu, J., Zhou, X., Wang, Y.H., Cheng, X., Li, P.*, et al.* (2011). The ubiquitin ligase Peli1 negatively regulates T cell activation and prevents autoimmunity. Nat. Immunol. *12*, 1002-1009.

Fernandez, M., Porosnicu, M., Markovic, D., and Barber, G.N. (2002). Genetically engineered vesicular stomatitis virus in gene therapy: application for treatment of malignant disease. J. Virol. *76*, 895-904.

Maggirwar, S.B., Harhaj, E.W., and Sun, S.-C. (1997). Regulation of the interleukin-2 CD28 responsive element by NF-ATp and various NF-κB/Rel transcription factors. Mol. Cell. Biol. *17*, 2605-2614.

Mallette, F.A., and Richard, S. (2012). JMJD2A promotes cellular transformation by blocking cellular senescence through transcriptional repression of the tumor suppressor CHD5. Cell Rep. *2*, 1233-1243.

Stojdl, D.F., Lichty, B.D., tenOever, B.R., Paterson, J.M., Power, A.T., Knowles, S., Marius, R., Reynard, J., Poliquin, L., Atkins, H.*, et al.* (2003). VSV strains with defects in their ability to shutdown innate immunity are potent systemic anti-cancer agents. Cancer Cell *4*, 263-275.